Exploiting time varying sparsity for underwater acoustic communication via dynamic compressed sensing

Weihua Jiang,[1] Siyuan Zheng,[1] Yuehai Zhou,[1] F. Tong,[1,a)] and Ryan Kastner[2]
[1]*The Key Laboratory of Underwater Acoustic Communication and Marine Information Technology of the Minister of Education, Xiamen University, Xiamen, Fujian, 361005, China*
[2]*Department of Computer Science and Engineering, University of California San Diego, La Jolla, California 92093, USA*

(Received 7 December 2017; revised 14 May 2018; accepted 16 May 2018; published online 29 June 2018)

While it has been recognized that the multipath structure of the underwater acoustic (UWA) channel offers the potential for compressed sensing (CS) sparsity exploitation, the rapidly time varying arrivals induced by highly dynamic surfaces unfortunately pose significant difficulties to channel estimation. From the viewpoint of underwater acoustic propagation, with the exception of the highly time varying arrivals caused by dynamic surface, generally there exist relatively stationary or slowly changing arrivals caused by direct path or bottom reflection, which imply the adoption of a discriminate estimation method to handle sparse components with different time variation scale. By modeling the time varying UWA channels as a sparse set consisting of constant and time-varying supports, in this paper, estimation of time varying UWA channel is transformed into a problem of dynamic compressed sensing sparse recovery. The combination of a Kalman filter and compressed sensing is adopted to pursue the solution of it. Numerical simulations demonstrate the superiority of the proposed algorithm. In the form of a channel-estimation-based decision-feedback equalizer, the experimental results with the field data obtained in a shallow water acoustic communication experiment indicate that the proposed dynamic compressed sensing algorithm outperforms classic algorithms as well as CS algorithms.
https://doi.org/10.1121/1.5042355

[CFM] Pages: 3997–4007

I. INTRODUCTION

The technology of underwater acoustic communication has drawn extensive attention from rapidly growing marine missions such as underwater sensor network, environmental monitoring, bottom engineering, and resource exploitation.[1,2] The nature of the ocean environment unfortunately creates a complicated multi-path communication channel, which simultaneously exhibits large delay spreads as well as fast time variations and thus poses significant difficulties to the estimation and equalization of the underwater acoustic (UWA) channel.[3–5] It has been well recognized by the research community that the sparse structure of the UWA channel—i.e., there only exist a few multipath arrivals within the large time delay spread—can be used to improve the estimation performance.[6,7]

Compressed sensing (CS) has found rapidly increasing applications in areas of applied mathematics, computer science, and signal processing.[8] Most of the conventional compression perception reconstruction algorithms are designed to address the static sparse signal reconstruction;[9–11] namely, the coordinates and amplitudes of non-zero elements in the signal and the measurement matrix do not change with time. Among them, the smoothed l_0-norm approach[12,13] has been popularly investigated to explore the sparse feature of multipath channel.

However, in the sparse estimation of time varying UWA channel, both amplitude and delay of the arrivals experience time variations. As a result, under the classic CS framework the corresponding support set and measurement matrix also exhibits dynamic change.[1] Nonetheless, existing solutions for the dynamic problem[14,15] treat the entire time sequence as a single spatiotemporal signal and perform CS to reconstruct it. It is a batch solution (it is necessary to wait to get the entire observation sequence), and thus suffers from a high computational complexity.[16]

Another type of sparse estimation strategy performs the thresholding operation on the channel coefficients obtained with a classic channel estimation algorithm such as Least Square (LS)[17–19] to directly set small taps to zero. However, the exact threshold for distinguishing the non-zero taps is difficult to determine for the time varying channels.

Greedy methods, such as matching pursuit (MP)[20] and orthogonal matching pursuit (OMP)[21] algorithms are important sub-branches of the l_1-norm CS method. While the MP algorithm computes adaptive signal representations with a dictionary of Gabor functions, the OMP algorithm is designed to project the orthogonal component of the signal onto the set of atoms selected to achieve better results.[21] It is recognized that the OMP algorithm provides similar recovery performance but with less complexity when compared to the basis pursuit (BP) method.[22]

However, the OMP algorithm is subject to performance degradation caused by time varying sparsity, as the time

a)Electronic mail: ftong@xmu.edu.cn

variation will significantly deteriorate the correlation between the signal vectors and the required atoms. As the dynamic propagation phenomena such as scattering from rough surfaces will cause diffuse multipath patterns, which can be properly modeled by a block sparse channel instead of a purely sparse one, the block-orthogonal matching pursuit (BOMP) algorithm has been proposed to address this type of dynamic sparsity.[23,24]

As the Delay-Doppler spread function is capable of converting the time varying sparse structure at time domain into a more stable Delay-Doppler representation,[25] channel estimation approaches based on the Delay-Doppler spread function are attractive for estimating rapidly time varying channels. Previous investigations that addressed the optimization of Delay-Doppler channel model with OMP algorithm[25] or basis expansion models[26] have been reported. However, as the whole channel response needs to be formulated with the Delay-Doppler model, for channels with large delay spread, this type of estimation algorithm will suffer from huge computational complexity in order to resolve the sparse solution over an extremely large two-dimensional searching space. Moreover, it has been recognized that, with the exception of highly time varying arrivals caused by dynamic surface, generally there exist relatively stationary or slowly changing arrivals caused by direct path or bottom reflection, which imply the adoption of discriminate estimation methods to address sparse components with different time variations instead of Delay-Doppler searching for all the multipath arrivals.

Dynamic compressed sensing (DCS) is a novel branch of CS theory for recovery of a compressible—possibly with a slowly varying sparsity pattern—signal from a time sequence of noisy observations.[16] It has found extensive application in the area of video signal processing, dynamic nuclear magnetic resonance imaging, dynamic target detection, and sensor data fusion.[27–30] Nevertheless, until now, limited efforts have been reported in using DCS for the estimation of time varying UWA channel.[27]

In recent works,[16,28] the problem of causally reconstructing time sequences of spatially sparse signals with unknown and slow time varying sparsity patterns from a limited number of linear "incoherent" measurements were studied by a solution called Kalman Filtered Compressed Sensing (KF-CS). The key idea here is to run a reduced order Kalman filter[27] (KF) only for the current signal's estimated nonzero coefficients' set, while performing CS on the error of Kalman filtering error to estimate new additions, if any, to the set. Note that, while it is common to use a KF to fit channel variation with the optimum linear recursion, the classic KF is unfortunately not capable of utilizing the sparse feature of multipath channel.[31]

In Ref. 32, the Dantzig selector (DS)[33–35] is applied to estimate new additions by transforming the selection of the best subset of variables into the solving of a very simple convex program, which, in fact, can easily be recast as a convenient linear program (LP). However, solving the linear programming problem requires a high computational complexity,[36] which is greatly limiting its practical application.

Motivated by the successful applications of DCS method,[16,28] in this paper, KF-CS estimation of the time varying underwater acoustic channel is investigated. Different from the previous DCS work in which the DS is transformed into a linear programming problem,[16,28] in this paper, the Primal Dual Pursuit (PD-pursuit)[37,38] method is adopted for the DS to solve the complex-valued convex optimization problem. Finally, for performance evaluation and comparison, we applied the KF-CS channel estimation algorithm to drive a channel estimate based decision feedback equalizer (CE-DFE)[39] in the context of an experimental UWA communication system for performance evaluation and comparison.

The contributions of this study are listed as follows. First, by converting the estimation of time varying UWA channel into a DCS problem, the dynamic compressed sensing algorithm is designed for the UWA channel that simultaneously exhibits large delay spread and fast time variations. Second, based on numerical simulations, we provide performance comparisons among the OMP, smoothed l0 estimation (SL0),[12,13] BOMP,[23,24] linear Kalman estimation (Kalman),[31] Least Square QR-factorization (LSQR)[19] algorithm, as well as the proposed KF-CS algorithm. Furthermore, field data obtained from a physical shallow water channel is adopted to assess the impacts of different channel estimation algorithms on the UWA communication performance.

The paper is organized as follows. Section II formulates the sparse acoustic channel model and poses the problem of compressive sensing channel estimation. Section III presents the proposed KF-CS algorithm and its theoretical performance analysis. Section IV provides the numerical simulations. Section V contains the results and an analysis of the field experiment. Finally, we provide conclusions in Sec. VI.

II. PROBLEM FORMULATION

A. System model

In this paper, we use bold capital (lower case) letters to denote matrices (vectors). Superscripts *, $'$, and ^{H} denote complex conjugate, transpose, and Hermitian, respectively; Notation 1 or 0 means all elements in the vector of appropriate size are one or zero; Notation $||\mathbf{a}||$ is the l_2 norm (Euclidean norm) of the vector $\mathbf{a}$. Notation $\|\mathbf{a}\|_1$ refers to the l_1 norm, which is the sum of the absolute value of each vector element; Notation $\|\mathbf{a}\|_0$ denotes the l_0 pseudo-norm, which is the number of non-zero elements in the vector. Notation $\mathbf{A}^\dagger$ represents the matrix pseudo inverse. $CN(\mathbf{a},\mathbf{B})$ denotes the complex Gaussian vector with mean $\mathbf{a}$ and covariance matrix $\mathbf{B}$.

The discrete input-output representation of a communication system can be written as[7]

$$y[i] = \sum_{j=0}^{N-1} s^*[i-j]h[j] + w[i], \quad i = 0, ..., M-1, \tag{1}$$

where $s[i]$, $y[i]$, and $w[i]$ are the discrete transmitted signal, received signal, and additive white noise at time i, respectively, and $h[j]$ is channel impulse response with a length of N. In Eq. (1), M is the observation length for channel

estimation. Note that the underwater acoustic channel is assumed to remain static during the observation period.[7,25]

Equation (1) can be expressed in matrix form as

$$\mathbf{y} = \mathbf{A}\mathbf{h} + \mathbf{w}, \tag{2}$$

where $\mathbf{y} \in C^{M\times 1}$, $\mathbf{h} \in C^{N\times 1}$, and $\mathbf{w} \in C^{M\times 1}$ are the vector form of the received signal, impulse response function, and additive white noise, respectively. The measurement matrix or the convolution matrix, $\mathbf{A} \in C^{M\times N}$, is constructed from the transmitted signal as shown in Eq. (3),

$$\mathbf{A} = \begin{bmatrix} s^*[0] & s^*[-1] & \cdots & s^*[-N+1] \\ s^*[1] & s^*[0] & \cdots & s^*[-N+2] \\ \vdots & \vdots & & \vdots \\ s^*[M-1] & s^*[M-2] & \cdots & s^*[M-N] \end{bmatrix}. \tag{3}$$

It is straightforward that estimation of $\mathbf{h}$ in Eq. (2) can be transformed to a CS problem of pursuing the sparse solutions of $\mathbf{h}$ with the sparsity factor κ, which is defined as the number of non-zero elements in the channel response $\mathbf{h}$. According to Ref. 40, to obtain the unique sparse solution of Eq. (2), the measurement matrix $\mathbf{A}$ should satisfy the restricted isometry property (RIP)

$$(1-\delta_{2\kappa})||\mathbf{h}||_2^2 \le ||\mathbf{A}\mathbf{h}||_2^2 \le (1+\delta_{2\kappa})||\mathbf{h}||_2^2, \tag{4}$$

where $\delta_{2\kappa}$ is a constant related to the sparsity of 2κ. If $\delta_{2\kappa} \ll 1$, the measurement matrix $\mathbf{A}$ has a large probability to reconstruct the κ sparse signal $\mathbf{h}$ stably.

B. Performance metrics

The received signal-to-noise ratio (SNR), $\rho_{\mathbf{y}}$, is defined as

$$\rho_{\mathbf{y}} = 10\log_{10}\frac{||\mathbf{A}\mathbf{h}||_2^2}{||\mathbf{w}||_2^2}. \tag{5}$$

If the impulse response is known, the performance of the channel estimation can be quantitatively measured by the channel recovery SNR (ρ_{CR}) in dB,

$$\rho_{CR} = 10\log_{10}\frac{||\mathbf{h}||_2^2}{||\mathbf{h}-\tilde{\mathbf{h}}||_2^2}, \tag{6}$$

where $\tilde{\mathbf{h}}$ is the estimated impulse response.

As the physical impulse response associated with the field data is unknown, to further assess the performance of the different channel estimation methods, the CE-DFE[39] is employed to recover the transmitted sequence. The bit error rate (BER) of the equalizer acts as performance metric for channel estimation from the viewpoint of underwater acoustic communication.

III. KF-CS

The idea of KF-CS[16,27–30] reconstruction for a sparse signal sequence with varying support can be briefly introduced as follows.

The measurement model is

$$\mathbf{y}_t = \mathbf{A}\mathbf{h}_t + \mathbf{w}_t,\ \mathbf{w}_t \sim CN(0, \sigma_{obs}^2\mathbf{I}), \tag{7}$$

where $\mathbf{y}_t, \mathbf{h}_t, \mathbf{w}_t$ are the vector form of the received signal, impulse response function, and addictive noise. $\mathbf{A} \in C^{n\times m}$ is the measurement matrix, with $n < m$. n and m are the length of the received signal $\mathbf{y}_t$ and impulse response $\mathbf{h}_t$ respectively. σ_{obs}^2 is the variance of observation noise. Our goal is to get the estimate $\mathbf{h}_t$ at each t. Let $\hat{\mathbf{h}}_{t|t-1}, \hat{\mathbf{h}}_t, \mathbf{P}_{t|t-1}, \mathbf{P}_t$ and $\mathbf{K}_t$ denote the predicted and updated state estimates, the prediction and updated error covariances at time t, and the Kalman gain given by the KF in KF-CS, respectively. Let N_t denote the support set of $\mathbf{h}_t$, $T_t = \hat{N}_t$ denote its estimate, and T^c denote the complement of T, i.e., $T^c = [1:m]\backslash T$. In addition, let Δ_t denote the undetected nonzero set at time t, i.e., $\Delta_t = N_t\backslash T_{t-1}$, and $\tilde{\Delta}_t$ denote its estimate.

As the nonzero coefficients' set N_t changes slowly over time, for the currently nonzero coefficients of $\mathbf{h}_t$, $(\mathbf{h}_t)_{N_t}$, we assume a spatially i.i.d. Gaussian random walk model, with noise variance σ_{sys}^2, while the rest of the coefficients remain constant, i.e., $\mathbf{h}_0 = 0, \mathbf{h}_t = \mathbf{h}_{t-1} + \mathbf{v}_t, \mathbf{v}_t \sim CN(0, \mathbf{Q}_t), \mathbf{Q}_t = \sigma_{sys}^2\mathbf{I}_{N_t}$. The new additions, if any, are estimated by performing CS on the Kalman filtering error $\tilde{\mathbf{y}}_{t,res}$. The variance of observation noise is assumed to be known as $\sigma_{obs}^2 = (\frac{1}{3}\sqrt{k/n})^2$ (taken from Refs. 16 and 32), where κ is the sparsity factor of the impulse response $\mathbf{h}_t$.

An approximate Maximum Likelihood (ML) is used to estimate σ_{sys}^2 from a training time sequence of signal $\mathbf{h}_1, \mathbf{h}_2 \ldots, \mathbf{h}_{L_{train}}$; here, L_{train} denotes the length of training sequence. By picking a threshold α to set all coefficients of $\mathbf{h}_t$ below it to zero and then using the rest of the coefficients to compute the ML estimate,[16,29] for $t = 1 : L_{train}$, if $|\mathbf{h}_{t,i}| < \alpha$, set $|\mathbf{h}_{t,i}| = 0$, where $\mathbf{h}_{t,i}$ is the ith entry of $\mathbf{h}_t$. And set the nonzero coefficients' set $\tilde{N}_t = \{i \in [1:m] : |\mathbf{h}_{t,i}| \ge \alpha\}$. Then the ML estimate is $\hat{\sigma}_{sys}^2 = \sum_{t=2}^{L_{train}} ||(\mathbf{h}_t - \mathbf{h}_{t-1})_{\tilde{N}_{t-1}}||_2^2 / \sum_{t=1}^{L_{train}} |\tilde{N}_t|$.

We explain the proposed KF-CS algorithm below.

(1) Running the Temporary KF: We first run a "temporary" Kalman prediction and update step using $\hat{\mathbf{Q}}_t = \hat{\sigma}_{sys}^2\mathbf{I}_{T_{t-1}}$, i.e., we compute

$$\begin{aligned} \mathbf{K}_{t,tmp} &= (\mathbf{P}_{t-1} + \hat{\mathbf{Q}}_t)\mathbf{A}'(\mathbf{A}(\mathbf{P}_{t-1} + \hat{\mathbf{Q}}_t)\mathbf{A}' + \sigma_{obs}^2\mathbf{I})^{-1}, \\ \hat{\mathbf{h}}_{t,tmp} &= (\mathbf{I} - \mathbf{K}_{t,tmp}\mathbf{A})\hat{\mathbf{h}}_{t-1} + \mathbf{K}_{t,tmp}\mathbf{y}_t. \end{aligned} \tag{8}$$

(2) Detecting and estimating the additions via CS: Let $T = T_{t-1}$ and $\hat{\mathbf{h}}_{t,tmp} = \hat{\mathbf{h}}_t$. The filtering error is

$$\begin{aligned} \tilde{\mathbf{y}}_{t,res} &= \mathbf{y}_t - \mathbf{A}\hat{\mathbf{h}}_{t,tmp} = \mathbf{A}_{T^c}(\mathbf{h}_t)_{T^c} + \mathbf{A}_T(\mathbf{h}_t - \hat{\mathbf{h}}_t)_T + \mathbf{w}_t \\ &= \mathbf{A}_{\Delta_t}(\mathbf{h}_t)_{\Delta_t} + \mathbf{A}_{(T\cup\Delta_t)^c}(\mathbf{0})_{(T\cup\Delta_t)^c} + \mathbf{A}_T(\mathbf{h}_t - \hat{\mathbf{h}}_t)_T + \mathbf{w}_t \\ &= \mathbf{A}_{\Delta_t}(\mathbf{h}_t)_{\Delta_t} + \mathbf{A}_T(\mathbf{h}_t - \hat{\mathbf{h}}_t)_T + \mathbf{w}_t, \end{aligned} \tag{9}$$

where $\mathbf{A}_{\Delta_t}$ and $\mathbf{A}_T$ denote the sub-matrix, obtained by extracting the columns of $\mathbf{A}$ corresponding to the undetected nonzero set at time t and the indices in T. To further improve the performance, we apply CS on the

residual from the KF, which is sparser than the original signal. The previous investigations of DCS[16,28] generally adopt the DS to detect the "non-compressible" nonzero set as

$$\tilde{\mathbf{y}}_{t,res} = \mathbf{A}\boldsymbol{\beta}_t + \mathbf{w}_t,$$
$$\hat{\boldsymbol{\beta}}_t = \arg\min_{\beta} \|\boldsymbol{\beta}\|_1, s.t. \|\mathbf{A}'(\tilde{\mathbf{y}}_{t,res} - \mathbf{A}\boldsymbol{\beta})\|_\infty \le \lambda_m \sigma_{obs},$$
$$\tilde{\Delta}_t = \{i \in T_{t-1}^c : \hat{\beta}_{t,i}^2 > \alpha_a\}, \tag{10}$$

where $\lambda_m = \sqrt{2\log m}, \boldsymbol{\beta}_t = [(\mathbf{h_t} - \hat{\mathbf{h}}_\mathbf{t})_T, (\mathbf{h})_{\Delta_t}, 0_{(T\cup\Delta_t)^c}]$ and α_a is the addition threshold. Thus, the estimated support set at time t is $T_t = T \cup \hat{\Delta}_t = T_{t-1} \cup \hat{\Delta}_t$.

Besides the huge computational burden caused,[41] as the linear program is designed for solving DS, it cannot handle complex-valued data.[16] While there are several methods for solving the complex data, such as DASSO (connections between the Dantzig selector and lasso), alternating direction method of multipliers (ADMM), Primal Dual Pursuit (PD-Pursuit), etc.,[36,42–44] compared to DASSO, the major advantage of PD-Pursuit is the direct computation of update directions. Meanwhile, the convergence of the ADMM algorithm requires the exact solution of the sub-problem.[43] Moreover, while the computational cost for a linear program is about $O(m^3)$,[41] the computational cost of PD-Pursuit algorithm is bounded by $O(d^* m^* n)$, where d is the total number of primal-dual steps taken and recover an S sparse signal from compressed measurements in at most S steps of primal dual update.[38] So, in terms of computational complexity the PD-Pursuit algorithm is also better than linear program and is thus adopted in this paper.

Under a primal-dual homotopy approach,[38] the implementation of the PD-Pursuit algorithm can be decomposed into two procedures: primal update and dual update. The DS solves the following primal program as

$$\min_{\beta} \|\boldsymbol{\beta}\|_1, s.t. \|\mathbf{A}'(\tilde{\mathbf{y}}_{t,res} - \mathbf{A}\boldsymbol{\beta})\|_\infty < \varepsilon. \tag{11}$$

The equivalent dual program representation of Eq. (11) is

$$\arg\max_{\gamma} -(\varepsilon\|\gamma\|_1 + \langle\gamma, \mathbf{A}'\tilde{\mathbf{y}}_{t,res}\rangle), s.t. \|\mathbf{A}'\mathbf{A}\gamma\|_\infty \le 1, \tag{12}$$

where $\gamma \in \mathbf{R}^n$ is dual vector. In primal update phase, it updates the primal vector and primal constraints which give the support and sign of dual vector. In dual update phase, it updates the dual vector and dual constraints which give the support and sign of the primal vector to be used in next primal update phase. We successively update the primal and dual variables at every step until we reach the solution point. And at every step, the update requires just a few matrix-vector multiplications.[38]

(3) KF-update: With the initialization of $\mathbf{P}_0 = 0_{[1:m],[1:m]}$, $\hat{\mathbf{h}}_0 = 0_{[1:m]}$, we run the Kalman prediction/update using $\hat{\mathbf{Q}}_t = \hat{\sigma}_{sys}^2 \mathbf{I}_{T_t}$

$$\mathbf{P}_{t|t-1} = (\mathbf{P}_{t-1} + \hat{\mathbf{Q}}_t),$$
$$\mathbf{K}_t = \mathbf{P}_{t|t-1}\mathbf{A}'(\mathbf{A}\mathbf{P}_{t|t-1}\mathbf{A}' + \sigma_{obs}^2\mathbf{I})^{-1},$$
$$\mathbf{P}_t = (\mathbf{I} - \mathbf{K}_t\mathbf{A})\mathbf{P}_{t|t-1},$$
$$\hat{\mathbf{h}}_t = (\mathbf{I} - \mathbf{K}_t\mathbf{A})\hat{\mathbf{h}}_{t-1} + \mathbf{K}_t\mathbf{y}_t. \tag{13}$$

(4) Deleting zero coefficients: If the addition threshold α_a is not large enough, alternatively some coefficients may be wrongly added due to CS error, which may be deleted as zero.

Finally the proposed KF-CS algorithm is described in Table I.

IV. NUMERICAL SIMULATION

In this section, numerical simulations are performed to demonstrate the effectiveness of the proposed KF-CS algorithm, compared with that of the sparse type OMP, BOMP, and SL0 algorithms, as well as the no sparsity exploitation Kalman and LSQR algorithms. A dynamic sparse underwater acoustic channel with complex-valued taps is artificially produced as the target channel. We consider a shallow water channel with a depth of 10 m and a distance of 500 m. The transmitter and the receiver are at the depth of 3 m and 5 m, respectively. Generated from the bell-hop[45] toolkit, the number of the non-zero taps is $\kappa = 6$ to present multipath arrivals as shown in Table II, the eigenrays associated with which are shown in Fig. 1. The length of the channel response is set as $N = 157$ with the equivalent sampling rate of 4000 Hz.

To artificially simulate the channel time variations induced by surface, two surface paths, i.e., path 2 and path 4, are imposed with additional time variations while the other four paths remain static. Specifically, delay of path 2 and path 4 is added with zero-mean random variations, while the corresponding magnitude is added with sinusoidal variations. The response of the simulated UWA channel with artificial time variations is presented in Fig. 2, from which we can see the different dynamic pattern of two surface paths.

Quadrature phase shift keying (QPSK) symbols with random distribution are generated to construct the measurement matrix A. The observation length for channel estimation is set

TABLE I. The proposed KF-CS.

Set $\hat{\mathbf{h}}_0, \mathbf{P}_0, T_0, \sigma_{obs}^2$

(1) Running the Temporary KF.
Run (8) using $\hat{\mathbf{Q}}_t = \hat{\sigma}_{sys}^2 \mathbf{I}_{T_{t-1}}$

(2) Detecting and estimating the Additions (using CS).
Compute $FEN = \tilde{\mathbf{y}}'_{t,res} \sum_{fe,t}^{-1} \tilde{\mathbf{y}}_{t,res}$ where $\tilde{\mathbf{y}}_{t,res} = \mathbf{y}_t - \mathbf{A}\hat{\mathbf{h}}_{t,tmp}$
If it is greater than its threshold, run CS on $\tilde{\mathbf{y}}_{t,res}$, the PD-pursuit algorithm is adopted for the DS.
Dual program is $\arg\max_{\lambda} -(\varepsilon\|\boldsymbol{\lambda}\|_1 + \langle\boldsymbol{\lambda}, \mathbf{A}'\tilde{\mathbf{y}}_{t,res}\rangle), s.t. \|\mathbf{A}'\mathbf{A}\boldsymbol{\lambda}\|_\infty \le 1$
The new estimated support is $T_t = T_{t-1} \cup \hat{\Delta}_t$

(3) KF-update.
Run (13) using $\hat{\mathbf{Q}}_t = \hat{\sigma}_{sys}^2 \mathbf{I}_{T_t}$.

(4) Deleting Zero Coefficients.

(5) Output.
solution of **h**.

TABLE II. Multipath delay and magnitude of the simulation UWA channel generated by bell-hop (Ref. 39).

	Nature of path	Time delay (ms)	Magnitude
Path 1	Direct path	6.7	$0.18 - 0.98j$
Path 2	Surface reflection	8.5	$0.67 + 0.36j$
Path 3	Direct path	10.5	$-0.22 - 0.19j$
Path 4	Surface reflection	13.8	$0.12 + 0.16j$
Path 5	Bottom reflection	16.0	$0.04 + 0.15j$
Path 6	Bottom reflection	19.8	$0.09 + 0.11j$

as $M = 100$ with the received SNR of $\rho_y = 30$ dB. The sparsity factor κ is assumed to be known in the KF-CS, BOMP, OMP, and the SL0 algorithm in the numerical simulation.

The other algorithm parameters of each algorithm are set by tuning to the best recovery SNR to facilitate performance evaluate. Specifically, for BOMP algorithm, the block size is 2; for SL0 algorithm, the iteration step size μ is 0.5;[12] for the Kalman algorithm, the noise variation is 0.002.

As the LSQR as well as the classic Kalman estimation algorithm will produce a large number of weak taps that are actually not existing in true impulse response, the OMP, SL0, BOMP, and KF-CS algorithms will be expected to achieve sparsity exploitation.

Shown in Fig. 3 is the recovery SNR achieved by different estimation methods. In particular, it is not surprising that all four sparse estimation algorithms, i.e., OMP, SL0, BOMP, and KF-CS, achieve significantly higher SNR than the LSQR and Kalman algorithm does. From Fig. 3, one may also notice that the Kalman estimator produces the worst SNR performance. This is because as both time delay and magnitude experience variations, the dynamics of time varying multipath arrival cannot be simply modeled by linear equation.

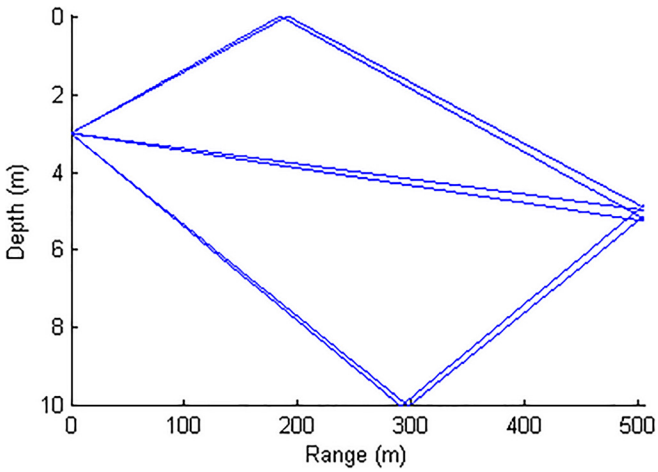

FIG. 1. (Color online) Eignerays of the simulated UWA channel.

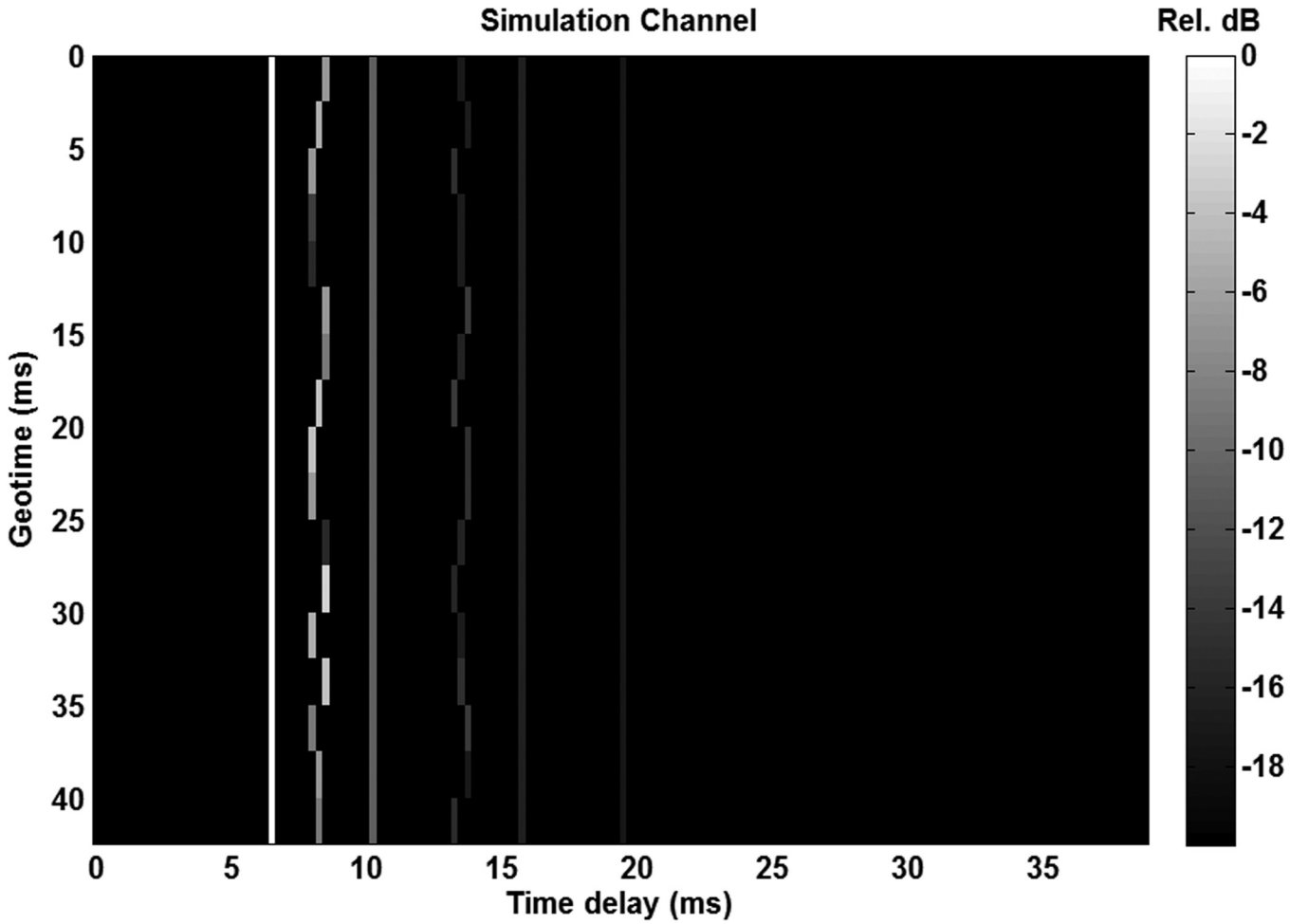

FIG. 2. Time varying response of the simulated UWA channel.

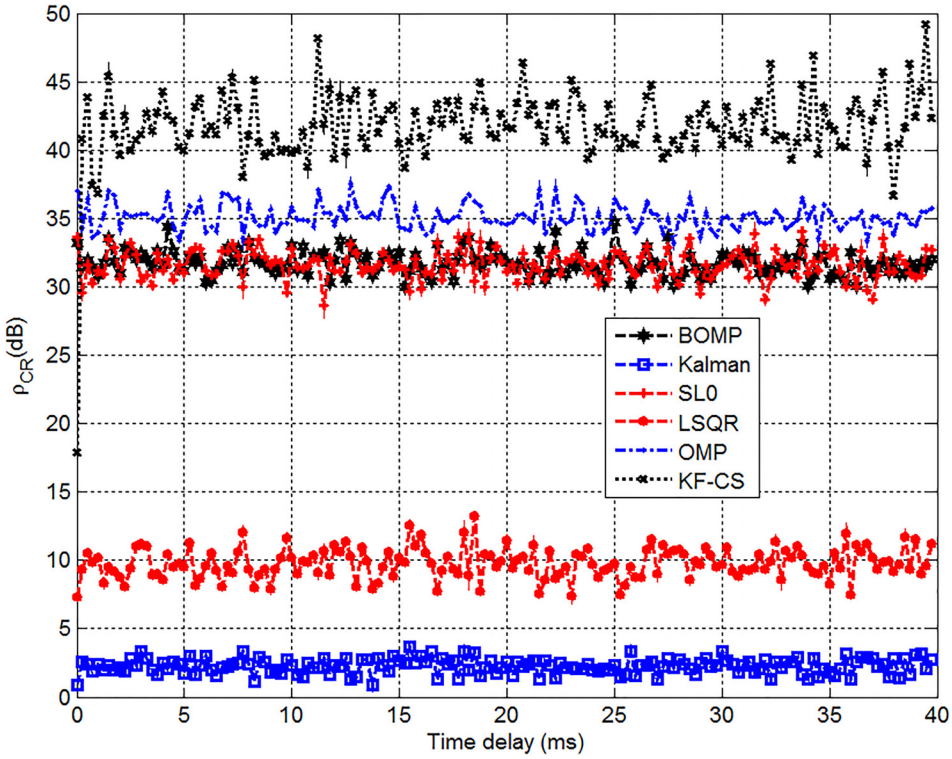

FIG. 3. (Color online) Channel recovery SNR ρ_{CR} (db) of different estimators.

As to four algorithms that are designed to utilize sparse feature, it is evident from the Fig. 3 that the proposed KF-CS algorithm outperforms the other three algorithms with the highest channel recovery SNR. While the OMP algorithm yields the second highest SNR, the BOMP and SL0 approach exhibit almost the same SNR curve. The result of numerical simulation in Fig. 3 implies that dynamic compressed sensing provides a promising way to explore time varying sparsity.

V. EXPERIMENTAL RESULTS AND DISCUSSION

A. CE-DFE for performance evaluation

As the accuracy of channel estimation will determine the performance of the resulting CE-DFE, in order to evaluate the performance of channel estimation, a CE-DFE is adopted to recover the transmitted symbol s in Eqs. (2) and (3) via[39]

$$\tilde{\mathbf{s}} = \mathbf{g}_{ff}\mathbf{y} + \mathbf{g}_{fb}\bar{\mathbf{s}}. \tag{14}$$

The decision output is

$$\bar{s}[i] = \mathrm{sgn}(\mathrm{real}(\tilde{s})) + \mathrm{j}^{*}\mathrm{sgn}(\mathrm{imag}(\tilde{s})). \tag{15}$$

In Eq. (14), for a feedback filter, $\bar{\mathbf{s}}$ is a vector of estimates of past transmitted data symbols, and the output of the filter is the soft decision estimate $\tilde{\mathbf{s}}$. In Eq. (15), the estimate $\tilde{\mathbf{s}}$ is the input to a decision device that generates the final estimate, $\bar{\mathbf{s}}$, of the transmitted data symbol. The feedforward and feedback filter, $\mathbf{g}_{ff}$ and $\mathbf{g}_{fb}$, are calculated as[39]

$$\mathbf{g}_{ff} = \frac{\mathbf{h}_0}{\mathbf{h}_0\mathbf{h}_0{}^{H} + \sigma_{\bar{n}}^2\mathbf{I} + \mathbf{H}_0\mathbf{H}_0^{H}}, \tag{16}$$

where $\sigma_{\bar{n}}^2 = ||\mathbf{y} - \mathbf{A}\tilde{\mathbf{h}}||_2^2$ and

$$\mathbf{g}_{fb} = -\mathbf{H}_{fb}\mathbf{g}_{ff}. \tag{17}$$

Here, $\mathbf{H}_0$, $\mathbf{h}_0$, and $\mathbf{H}_{fb}$ can be obtained from the convolution matrix $\mathbf{H}$, constructed from the impulse response estimate

$$\mathbf{H} = \begin{bmatrix} h[0] & \cdots & h[N-1] & \cdots & 0 \\ 0 & \cdots & h[N-1] & \cdots & 0 \\ & & \cdots & & \\ 0 & \cdots & h[0] & \cdots & h[N-1] \end{bmatrix} = [\mathbf{H}_0|\mathbf{h}_0|\mathbf{H}_{fb}]. \tag{18}$$

B. Field experiment

The experimental field data were collected from a shallow water acoustic channel at Wuyuan bay, Xiamen, China. The depth of the experiment area is about 9 m. The modulation format was QPSK with a bit rate of 4 kbps and a carrier frequency of 16 kHz. The signals were transmitted by a transducer suspended at a depth of 4 m under the pier, with a source level of about 185 dB re 1 μPa at 1 m. A four-element broad band receiver is mounted at the rear of an anchored ship covering from 2 to 6.5 m of the water column with an element spacing of 1.5 m. The distance of communication in the experiment is 1000 m as shown in Fig. 4(a). The sound velocity profile is provided in Fig. 4(b), which indicates a weak positive gradient.

Similar to the numerical simulation, the algorithm parameters of each algorithm are set by tuning to the best BER performance to facilitate performance evaluate. Specifically, for the BOMP algorithm, the block size is 2; for the SL0

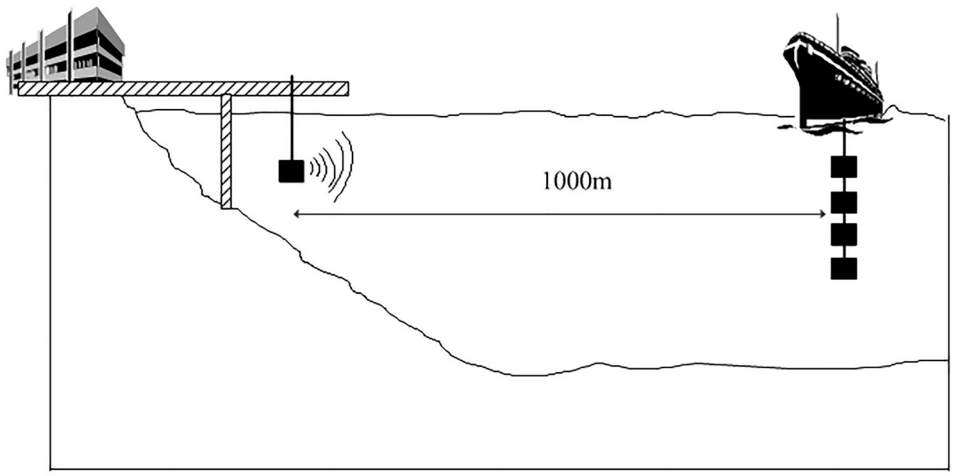

(a)

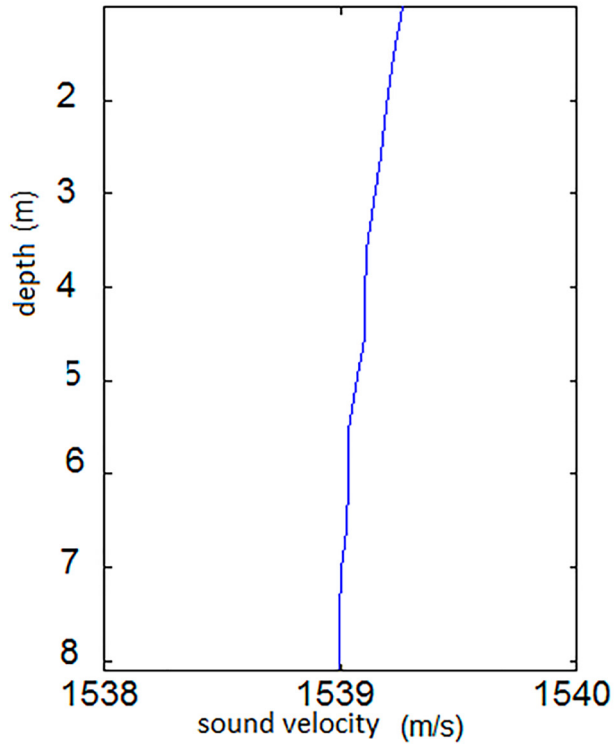

(b)

FIG. 4. (Color online) Setup of the field experiment and the corresponding sound velocity profile.

algorithm, the iteration step size μ is 0.7; for the Kalman algorithm, the noise variation is 0.02. The sparsity factor κ is set to 12, 12, 10, and 10 for the OMP, SL0, KF-CS, and BOMP algorithm, respectively.

The time varying response of the third UWA channel obtained by the five reference algorithms as well as the proposed KF-CS method, respectively, are shown in Fig. 5, which exhibits a multipath structure consisting of a cluster of strong arrivals and a rapidly varying arrival. Meanwhile, for two conventional estimation algorithms that do not utilize sparsity, substantial estimation noise in the time delay zone without multipath arrival is obvious. Furthermore, from Fig. 5, one may also observe that the KF-CS method achieves more dynamic details of the rapidly time-varying arrivals at the delay of approximate 7 ms compared to the other three sparse estimation methods.

C. Performance evaluation and comparison

The CE-DFE[39] is utilized for processing of the experimental data to evaluate the performance of the proposed KF-CS algorithm with the BER and constellation diagram adopted as the performance metrics.

For the CE-DFE driven by channel estimator, a periodic training strategy is adopted to address the time variation of the practical UWA channels. The data packet is divided into several data blocks. Each data block contains 300 known training symbols used for channel estimation and 900 information symbols that need to be recovered by the CE-DFE. The frame structure of QPSK packet is presented in Fig. 6. For each data block, after the channel estimation, the corresponding CE-DFE will produce BER values associated with this data block. The length of the channel estimator is set as $N = 80$, equivalent to

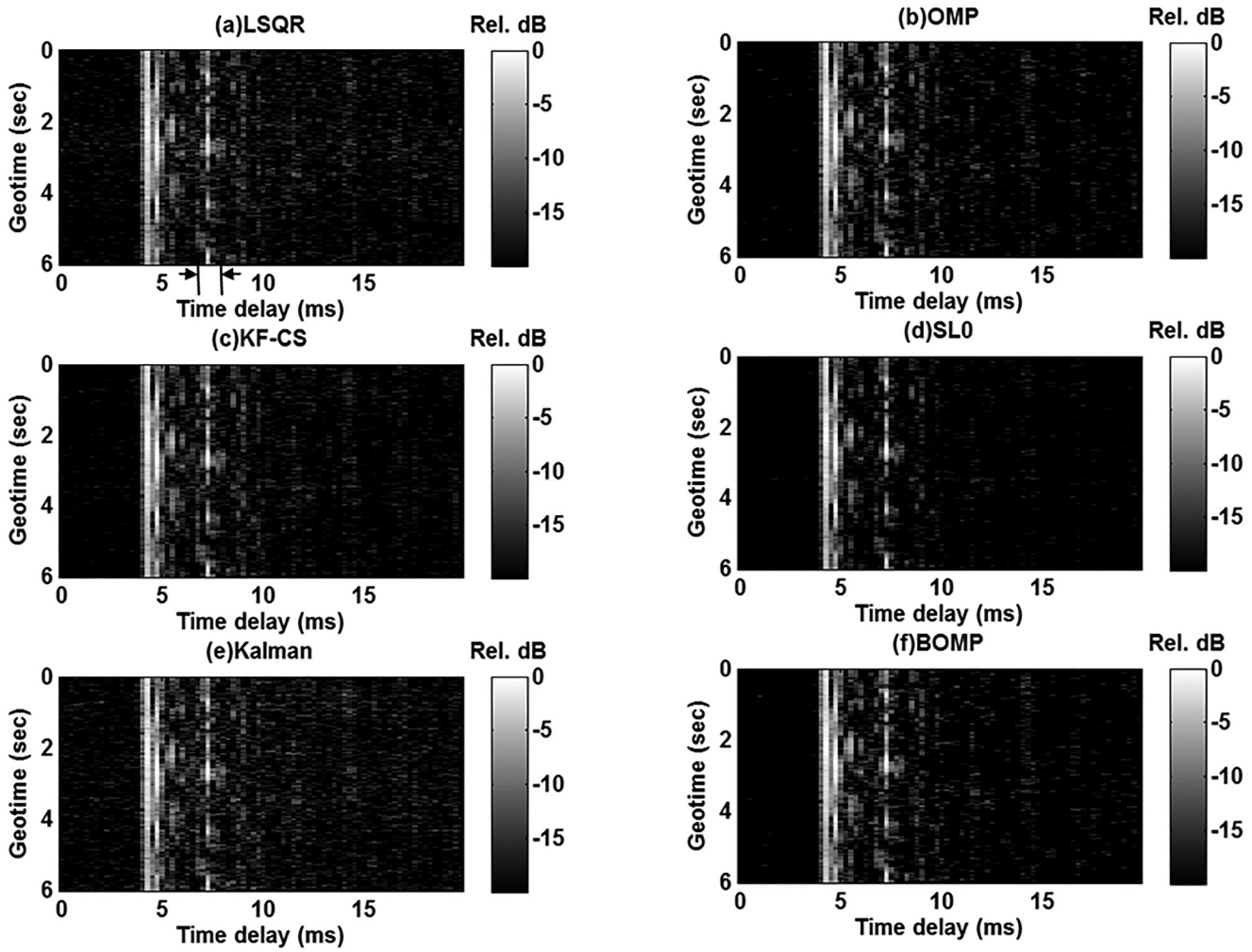

FIG. 5. Response of the third channel obtained by different methods.

20 ms. The residual error threshold for iteration termination is set as 4e-1. The channel estimation observation length is set as $M = 160$ symbols, equivalent to 40 ms. The lengths of the feedforward and feedback filter of decision feedback equalizer (DFE) are set as $N_{ff} = 160$ taps and $N_{fb} = 79$ taps, respectively. For each candidate algorithm, the above parameters are carefully selected to ensure the minimum BER.

The BER curves of the CE-DFE driven by different estimators are shown in Fig. 7(a). One may see that the KF-CS algorithm generates the lowest BER curve. Due to significant estimation noise in numerous near-zero taps as shown in Figs. 5(a)–5(e), the LSQR and Kalman estimator exhibit worse BER curves compared to the other four methods that explore sparse features.

Among the sparse estimation algorithms, the BOMP algorithm corresponds to a higher BER curve compared to the others. The reason may be that it is designed to achieve block sparse for all multipath arrivals, some of which are actually purely sparse instead of block sparse.

Note that, different from the simulation result in Fig. 3, the BER behavior of the SL0 method is superior to that of the OMP approach. It reveals that, compared with simulation that still contains some fixed multipath arrivals, the practical time-varying channel may lead to more impact on correction-based matching pursuit than on smooth l0 norm sparse recovery. In other words, smooth l0 norm provides a certain tolerance to time varying sparsity, as the multipath arrivals with varying time delay still contribute to sparse recovery.

Specifically, from Fig. 5, it is noticeable that, at the delay of approximate 7 ms, the presence of a highly time-varying multipath arrival unavoidably leads to significant impact on performance. To further investigate the BER performance of different estimation algorithms, estimated results on this multipath arrival are obtained by first normalizing the estimated channel response, and then accumulating the path energy within the time delay range of 2.5 ms [shown with arrows in Fig. 5(a)].

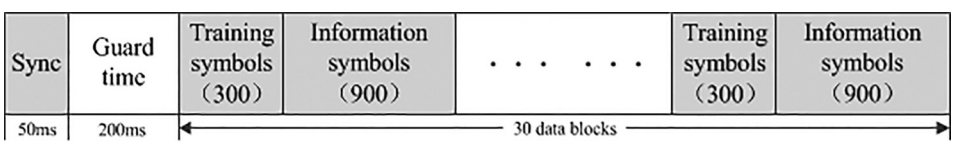

FIG. 6. The frame structure of the QPSK packet.

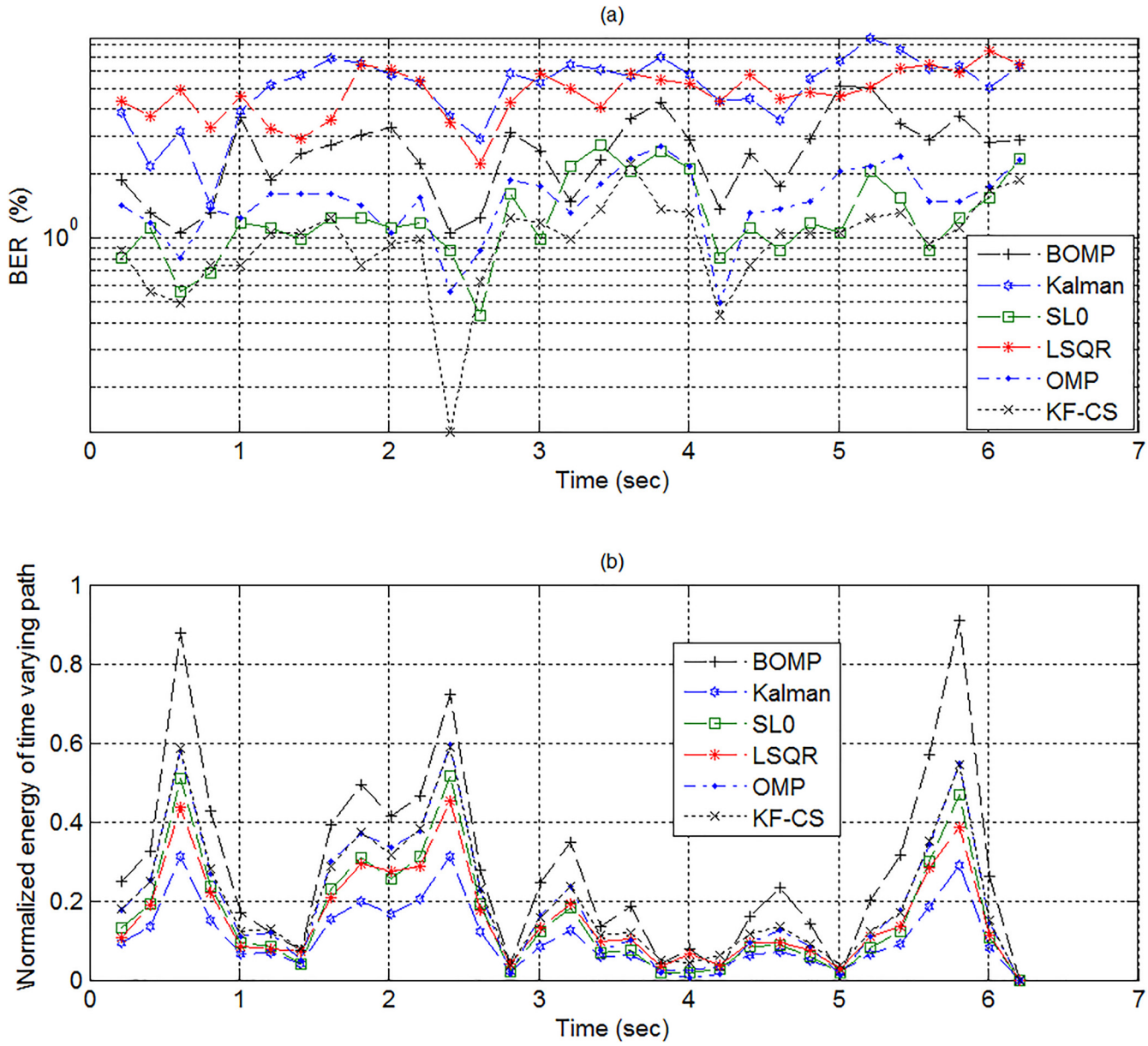

FIG. 7. (Color online) BERs of DEF (a), as well as the normalized energy of the time varying path (b).

With respect to the BER curves in Fig. 7(a), the estimated results on this time varying path are provided in Fig. 7(b) in terms of normalized energy. From Fig. 7(b), it can be concluded that, while the Kalman as well as LSQR algorithm exhibit under-estimation of this time varying path, the BOMP algorithm tends to overestimate this dynamic arrival as it is designed to achieve block sparsity on all sparse components. On the other hand, because OMP algorithm achieves matching pursuit by the means of cross-correlation, it experiences obvious performance degradation when the sparse component becomes extremely weak, as shown at the delay of 4 ms. Meanwhile, the SL0 algorithm also exhibits similar performance fluctuations with the time variation of multipath arrival. Under the framework of dynamic compressed sensing, note that the proposed algorithm achieves relatively stable performance with respect to the multipath time variation. Thus, the results in Fig. 7(b) partially contribute to clarifying the different BER behaviors in Fig. 7(a).

Regarding the average BER in terms of all the data blocks, as shown in Table III, the four estimators with sparsity exploitation generally outperform the two methods that do not exploit it. Specifically, while the average BER of LSQR and Kalman algorithm is 4.74% and 4.68%, the KF-CS algorithm yields an average BER of 1.01%, versus 1.47% by SL0 algorithm, 2.61% by BOMP, and 1.52% by OMP algorithm, respectively—the result of which is generally consistent with that of the BER curve in Fig. 7(a).

The constellation outputs associated with the different methods are provided in Fig. 8, from which one may observe

TABLE III. Averaged BER and ρ_{EO} value associated with three channel estimation algorithms.

Algorithm	LSQR	Kalman	OMP	BOMP	SL0	KF-CS
BER(%)	4.74	5.12	1.52	2.61	1.47	1.01

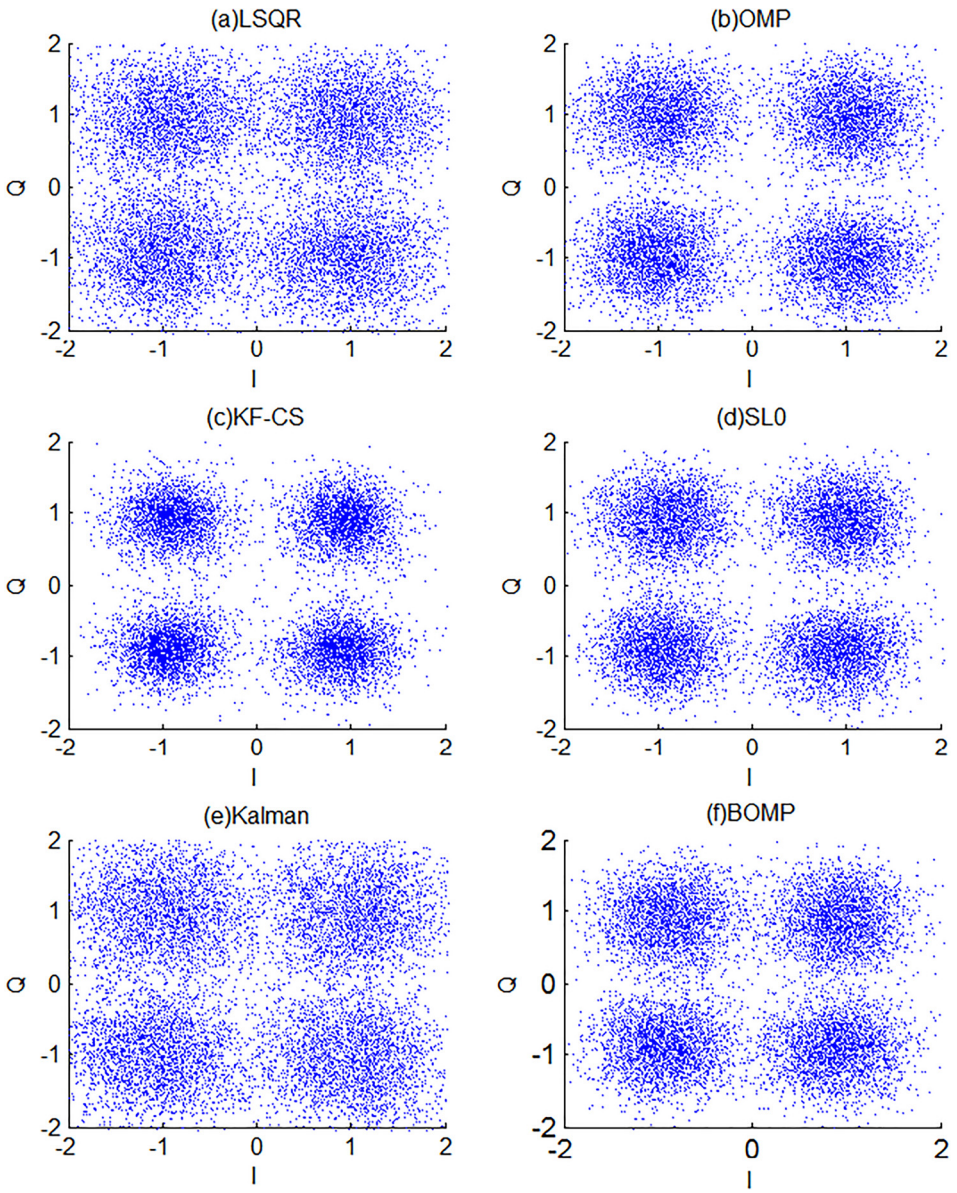

FIG. 8. (Color online) Constellation outputs of different channel estimators.

that the Kalman as well as LSQR estimator correspond to worse constellation quality due to considerable estimation noise. While the four sparse generally estimators achieve a better separating effect compared to the Kalman and LSQR method, from Fig. 8, it is evident that separability of the constellation associated with the other three sparse estimators is apparently inferior to that of the proposed KF-CS estimator. It can be attributed to the fact that, as the other three sparse methods are derived under the assumption that the sparse channel remains static, time variations of the UWA channel will inevitably lead to significant performance degradation. Thus, the comparison result of the constellation is also consistent with the BER result in Fig. 7(a).

VI. CONCLUSION

With the purpose to exploit the time varying sparsity, in this paper, the estimation of sparse UWA channel with time variations is investigated. As the UWA channel is treated as a sparse set with fixed support under the classic CS framework, the CS channel estimation strategies generally suffer from significant performance degradation at the presence of channel time variations.

By modeling the time varying UWA channel as sparse set with static supports as well as time varying supports, the problem of UWA channel estimation can be formulated under the DCS framework. Namely, with the running of a KF for estimation of the nonzero tap, sparse recovery is performed on the error of Kalman filtering to estimate new additions that produced by the time varying channel. Moreover, the PD-Pursuit algorithm for the DS is adopted to search for the complex domain KF-CS sparse solution.

The effectiveness of the proposed algorithm was first demonstrated by numerical simulations with artificially induced time variations. Finally, UWA communication experimental data were used to verify the proposed algorithm at the form of a CE-DFE, which indicates that the proposed KF-CS algorithm achieved the best performance compared to the conventional sparse or no sparsity exploitation algorithms.

ACKNOWLEDGMENT

The authors are grateful for the funding of the National Nature Science Foundation of China (Grants No. 11274259 and 11574258) in support of the present research.

[1]I. F. Akyildiz, D. Pompili, and T. Melodia, "Underwater acoustic sensor networks:Research challenges," Ad Hoc Networks **3**, 257–279 (2005).
[2]Y. H. Zhou, W. H. Jiang, F. Tong, and G. Q. Zhang, "Exploiting joint sparsity for underwater acoustic MIMO communications," Appl. Acoust. **116**, 357–363 (2017).
[3]M. S. Chitre, S. Shahabudeen, and M. Stojanovic, "Underwater acoustic communications and networking: Recent advances and future challenges," Mar. Technol. Soc. J. **42**, 103–116 (2008).
[4]A. C. Singer, J. K. Nelson, and S. S. Kozat, "Signal processing for underwater acoustic communications," IEEE Commun. Mag. **47**, 90–96 (2009).
[5]Y. H. Zhou, F. Tong, and G. Q. Zhang, "Distributed compressed sensing estimation of underwater acoustic OFDM channel," Appl. Acoust. **117**, 160–166 (2017).
[6]M. Stojanovic, "OFDM for underwater acoustic communications: Adaptive synchronization and sparse channel estimation," in *Proceedings of the International Conference on Acoustics, Speech, and Signal Processing*, Las Vegas, NV (March 30–April 4, 2008), pp. 5288–5291.
[7]M. Stojanovic, "Efficient processing of acoustic signals for high-rate information transmission over sparse underwater channels," Phys. Commun. **1**, 146–161 (2008).
[8]G. Kutyniok, *Compressed Sensing: Theory and Applications* (Cambridge University Press, Cambridge, UK, 2012), pp. 1289–1306.
[9]R. G. Baraniuk, "Compressive sensing [Lecture notes]," IEEE Signal Process. Mag. **24**, 118–121 (2007).
[10]D. L. Donoho, M. Elad, and V. N. Temlyakov, "Stable recovery of sparse overcomplete representations in the presence of noise," IEEE Trans. Inf. Theory **52**, 6–18 (2006).
[11]E. J. Candes, J. Romberg, and T. Tao, "Robust uncertainty principles: Exact signal reconstruction from highly incomplete frequency information," IEEE Trans. Inf. Theory **52**, 489–509 (2006).
[12]H. Mohimani, M. Babaie-Zadeh, and C. Jutten, "A fast approach for overcomplete sparse decomposition based on smoothed l0 norm," IEEE Trans. Signal Process. **57**, 289–301 (2009).
[13]G. Gui, Q. Wan, N. N. Wang, and C. Y. Huang, "Fast sparse multipath channel estimation with smooth l0 algorithm for broadband wireless communication systems," Commun. Netw. **3**, 1–7 (2011).
[14]M. Wakin, J. Laska, M. Duarte, D. Baron, S. Sarvotham, D. Takhar, K. Kelly, and R. Baraniuk, "An architecture for compressive imaging," in *Proceedings of the IEEE International Conference on Image Processing*, Atlanta, GA (October 8–11, 2006), pp. 1273–1276.
[15]U. Gamper, P. Boesiger, and S. Kozerke, "Compressed sensing in dynamic MRI," Magn. Reson. Med. **59**, 365–373 (2008).
[16]N. Vaswani, "Kalman filtered compressed sensing," in *Proceedings of the IEEE International Conference on Image Processing IEEE Xplore*, San Diego, CA (October 12–15, 2008), pp. 893–896.
[17]D. Middleton, "Channel modeling and threshold signal processing in underwater acoustics: An analytical overview," IEEE J. Oceanic Eng. **12**, 4–28 (1987).
[18]S. Cotter and B. Rao, "Sparse channel estimation via matching pursuit with application to equalization," IEEE Trans. Commun. **50**, 374–377 (2002).
[19]M. Jacobsen, P. C. Hansen, and M. A. Saunders, "Subspace preconditioned LSQR for discrete ill-posed problems," BIT Numer. Math. **43**, 975–989 (2003).
[20]S. G. Mallat and Z. Zhang, "Matching pursuits with time-frequency dictionaries," IEEE Trans. Signal Process. **41**, 3397–3415 (1993).
[21]J. A. Tropp and A. C. Gilbert, "Signal recovery from random measurements via orthogonal matching pursuit," IEEE Trans. Inf. Theory **53**, 4655–4666 (2007).
[22]J. A. Tropp, "Greed is good: Algorithmic results for sparse approximation," IEEE Trans. Inf. Theory **50**, 2231–2242 (2004).
[23]L. Y. Jing, C. B. He, J. G. Huang, and Z. Ding, "Joint channel estimation and detection using Markov chain Monte Carlo method over sparse underwater acoustic channels," IET Commun. **11**, 1789–1796 (2017).
[24]Y. C. Eldar, P. Kuppinger, and H. Bolcskei, "Compressed sensing for block-sparse signals: Uncertainty relations, coherence, and efficient recovery," IEEE Trans. Signal Process. **58**, 3042–3054 (2010).
[25]W. Li and J. C. Preisig, "Estimation of rapidly time-varying sparse channels," IEEE J. Oceanic Eng. **32**, 927–939 (2007).
[26]H. Yu, A. Song, M. Badiey, F. J. Chen, and F. Ji, "Iterative estimation of doubly selective underwater acoustic channel using basis expansion models," Ad Hoc Networks **34**, 52–61 (2015).
[27]N. Jing, W. H. Bi, Z. P. Hu, and L. Wang, "A survey on dynamic compressed sensing," Acta Autom. Sin. **41**, 22–37 (2015).
[28]N. Vaswani, "Analyzing least squares and Kalman filtered compressed sensing," in *Proceedings of the IEEE International Conference on Acoustics, Speech and Signal Processing*, Taipei, Taiwan (April 19–24, 2009), pp. 3013–3016.
[29]C. L. Qiu, W. Lu, and N. Vaswani, "Real-time dynamic MR image reconstruction using Kalman filtered compressed sensing," in *Proceedings of the IEEE International Conference on Acoustics, Speech and Signal Processing*, Taipei, Taiwan (April 19–24, 2009), pp. 393–396.
[30]J. Zhou, G. Xia, and J. Wang, "OFDM system channel estimation algorithm research based on Kalman filter compressed sensing," J. Theoret. Appl. Inf. Technol. **49**, 119–125 (2013).
[31]C. Komninakis, C. Fragouli, A. H. Sayed, and R. D. Wesel, "Multi-input multi-output fading channel tracking and equalization using Kalman estimation," IEEE Trans. Signal Process. **50**, 1065–1076 (2002).
[32]E. Candes and T. Tao, "The Dantzig selector: Statistical estimation when p is much larger than n," Ann. Stat. **35**, 2313–2351 (2007).
[33]V. M. Patel and R. Chellappa, "Sparse representation-based object recognition," in *Sparse Representations and Compressive Sensing for Imaging and Vision* (Springer, New York, 2013), pp. 63–84.
[34]X. L. Liu, X. Gong, and G. Y. Wang, "Face recognition based on linear representation model without residual estimation," CAAI Trans. Intell. Syst. **9**, 285–291 (2014).
[35]F. Li, L. Lin, and Y. Su, "Variable selection and parameter estimation for partially linear models via Dantzig selector," Metrika **76**, 225–238 (2013).
[36]V. Koltchinskii, "The Dantzig selector and sparsity oracle inequalities," Bernoulli **15**, 799–828 (2009).
[37]S. C. Billups, "A homotopy-based algorithm for mixed complementarity problems," SIAM J. Optim. **12**, 583–605 (2002).
[38]M. S. Asif, "Primal dual pursuit: A homotopy based algorithm for the Dantzig selector," Master's thesis, Georgia Institute of Technology, Atlanta, GA, 2008.
[39]J. C. Preisig, "Performance analysis of adaptive equalization for coherent acoustic communications in the time-varying ocean environment," J. Acoust. Soc. Am. **118**, 263–278 (2005).
[40]C. R. Berger, Z. Wang, J. Huang, and S. Zhou, "Application of compressive sensing to sparse channel estimation," IEEE Commun. Mag. **48**, 164–174 (2010).
[41]E. J. Candes and T. Tao, "Decoding by linear programming," IEEE Trans. Inf. Theory **51**, 4203–4215 (2005).
[42]G. M. James, P. Radchenko, and J. Lv, "DASSO: Connections between the Dantzig Selector and Lasso," J. R. Stat. Soc. **71**, 127–142 (2009).
[43]K. Frick, P. Marnitz, and A. Munk, "Statistical multiresolution Dantzig estimation in imaging: Fundamental concepts and algorithmic framework," Electron. J. Stat. **6**, 231–268 (2012).
[44]L. Li, Y. Li, and Q. Ling, "Fast algorithms to solve the Dantzig selector," in *Proceedings of the IEEE International Conference on Control and Automation*, Hangzhou, China (June 12–14, 2013), pp. 1544–1549.
[45]S. Kostas, C. Paolo, and Z. Michele, "The throughput of underwater networks: Analysis and validation using a ray tracing simulator," IEEE Trans. Wireless Commun. **12**, 1108–1117 (2013).